

Pressure induced suppression of the singlet insulator phase in BaVS₃: infrared optical study

I. Kézsmárki and G. Mihály

*Electron Transport Research Group of the Hungarian Academy of Science and Department of Physics,
Budapest University of Technology and Economics, 1111 Budapest, Hungary*

R. Gaál, N. Barišić, H. Berger, and L. Forró

Institut de Physique de la matière complexe, EPFL, CH-1015 Lausanne, Switzerland

C.C. Homes

Department of Physics, Brookhaven National Laboratory, Upton, New York 11973

L. Mihály

Department of Physics, State University of New York at Stony Brook, Stony Brook, New York 11794-3800

(Dated: version March 22, 2002)

The metal-insulator (MI) transition in BaVS₃ has been studied at ambient pressure and under hydrostatic pressure up to $p = 26$ kbar in the frequency range of $20 - 3000 \text{ cm}^{-1}$. The charge gap determined from the optical reflectivity is enhanced, $\Delta_{ch}(p)/k_B T_{MI}(p) \sim 12$. This ratio is independent of pressure indicating that the character of the transition does not vary along the $p-T$ phase boundary. Above the critical pressure, $p_{cr} \sim 20$ kbar, metallic spectra were recorded in the whole temperature range, as expected from the shape of the phase diagram. Our results exclude the opening of a pseudogap above T_{MI} at any pressure. Below T_{MI} an unusually strong temperature dependence of the charge gap was observed, resulting in a $\Delta_{ch}(T)$ deviating strongly from the mean field-like variation of the structural order parameter.

A class of symmetry breaking phase transitions, characterized by an anomalously large gap parameter, has recently attracted much attention and has been investigated intensely in the wider framework of strongly correlated electron systems. Though in some manganites and nickelates the huge enhancement of the $\Delta/k_B T_c$ ratio, sometimes as large as ~ 30 , is accompanied by the opening of a pseudogap above T_c [1, 2], in most cases a mean-field-like temperature dependence of Δ is observed. In contrast, in first order metal-insulator transitions a more drastic, often discontinuous opening of the charge gap is seen. On the other hand, the transition in the inorganic spin-Peierls system CuGeO₃ looks almost like a first order one, as the opening of the singlet-triplet gap is much sharper than the BCS functional form and follows $\Delta \propto (T_c - T)^\beta$ with $\beta \approx 0.1$ instead of 0.5 [3]. In BaVS₃, the detailed temperature dependence of neither the spin gap nor the charge gap has been measured so far. The present study of the infrared (IR) optical properties demonstrates that electron correlations play crucial role in BaVS₃: they lead to a large enhancement of the $\Delta/k_B T_c$ ratio and simultaneously give rise to an abrupt temperature dependence of Δ .

At ambient pressure BaVS₃ exhibits a phase transition from a high-temperature paramagnetic “bad metal” phase to a low-temperature singlet insulator state at $T_{MI} \approx 70$ K [4]. This is a second order phase transition, as it has been pointed out recently by the comparison of the anomalies observed in different thermodynamic properties [5]. The observation of the crystal symmetry lower-

ing [6] in more recent X-ray experiments provided direct evidence for the second order character of the transition at $T_{MI} \approx 70$ K.

The metallic nature of the compound is enhanced by the application of hydrostatic pressure and the transition temperature is suppressed at an average rate of $\Delta T_{MI}/\Delta p \approx 3.4 \text{ K/kbar}$ [7, 8]. The critical pressure above which the metallic phase extends over the whole temperature range is $p_{cr} \approx 20$ kbar [8]. The suppression of the insulating phase is accompanied by a monotonic decrease of the spin gap [5]. Moreover, the phenomenon occurring at $T_{MI} \approx 70$ K at ambient pressure has been described as a spin-Peierls-like transition. Its order parameter, Δ_{sp} , scales with the transition temperature as a function of pressure according to $\Delta_{sp}/k_B T_{MI} \approx 3.6$ [9]. This indicates that the character of the phase transition does not change under pressure.

Dc conductivity measurements clearly demonstrate the opening of a charge gap (Δ_{ch}) [10]. However, the magnitude and temperature dependence of Δ_{ch} can not be determined unambiguously: the purity of the sample has a strong influence on the transport in the insulating phase, and the activation energy obtained from the dc conductivity is temperature dependent. The results vary between $\Delta_{ch} = 570$ K and 1120 K [7, 11]. The photoemission threshold energy obtained by Nakamura *et al.* [11] corresponds to an intermediate value, $\Delta_{ch} \approx 710$ K. The present IR optical study reveals the magnitude and temperature dependence of the charge gap at ambient pressure. We also find that the $\Delta_{ch}/k_B T_{MI}$ ra-

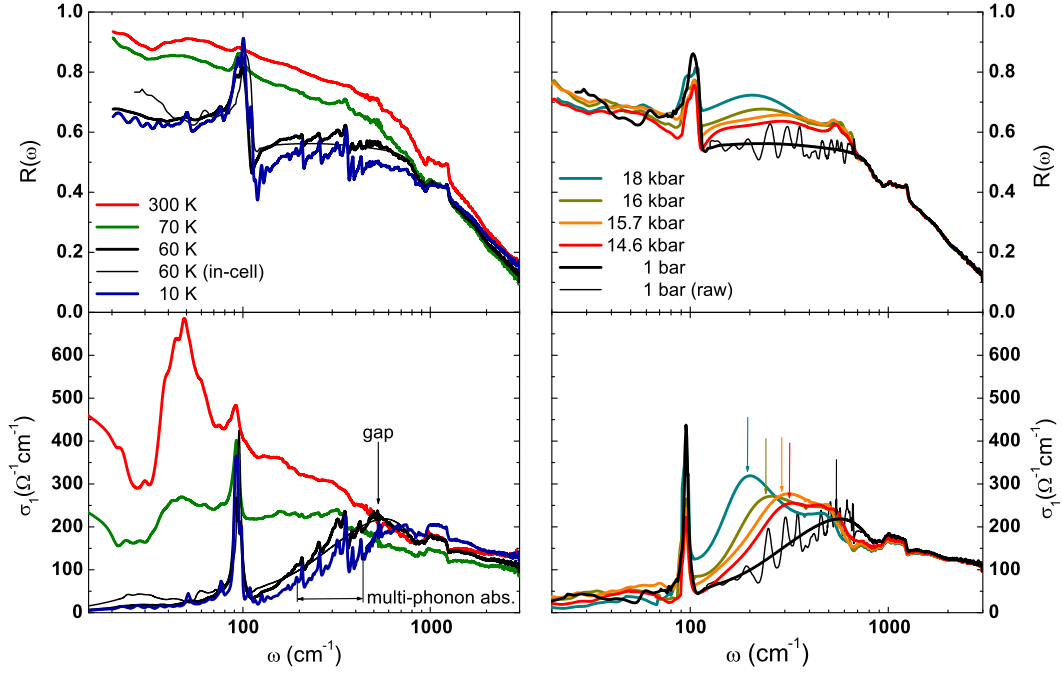


FIG. 1: Left: The reflectivity and conductivity spectra of BaVS₃ at ambient pressure as a function of temperature. The value of the gap and the multi-phonon branch just below the gap are indicated by arrows. For comparison the data obtained at $T = 60$ K inside of the pressure cell are also plotted. Right: The reflectivity and conductivity spectra in the insulating phase of BaVS₃ at several pressures. The arrows indicate the frequencies identified with the gap values. At ambient pressure both the raw spectra (evaluated by Eq. 1) and the smoothed curves are shown.

tio is independent of pressure. However, in contrast to $\Delta_{sp}/k_B T_{MI}$, that is very close to the BCS ratio, the measured $\Delta_{ch}/k_B T_{MI}$ is 3 times larger. The charge gap represents a higher energy scale in the system.

Infrared reflectivity of BaVS₃ single crystals has been measured in the frequency range of $\omega = 20 - 3000$ cm⁻¹, between room temperature and 10 K, at several pressures up to $p = 26$ kbar. The incident light was unpolarized, and nearly perpendicular to the rectangular (1 mm \times 3 mm), cleaved surface of the sample. Since the small spotsize of the beam and the high intensity in the FIR range were crucial requirements for this study most of the measurements were done at the U10A beamline of the National Synchrotron Light Source of the Brookhaven National Laboratory, with a Bruker 66v/S spectrometer. At ambient pressure the sample was mounted on the cold finger of a helium flow cryostat. The reflectivity data were referenced to the reflectivity of a gold mirror, also mounted on the cryostat. Some of the data below 50 cm⁻¹ were taken in a Bruker 113v spectrometer, using the internal source, with a Au film evaporated to the surface of the sample to act as a reference. The same crystal was also studied in a custom designed self-clamping pressure cell. Optical access was achieved through a cylindrical natural diamond, with wedged plane surfaces to eliminate interference fringes, and to facilitate reference measurements. The large (1.5 mm) window size and the ab-

sence of low-frequency absorption allowed investigations down to 20 cm⁻¹. We used the light reflected from the outer surface of the diamond (vacuum-diamond boundary) as a reference signal. The sample was mounted on the inner surface of the diamond, and the angle of wedging between the two surfaces allowed for a clean separation of the reference and sample reflection. Besides the optical access, an electrical leadthrough was also implemented, and the pressure was monitored *in situ* by an InSb sensor. The pressure cell was also cooled by the He flow cryostat.

The left panel in Fig. 1 summarizes the evolution of the optical spectra as a function of temperature at ambient pressure. The evaluation of the spectra in the pressure cell, shown in the right panel of Fig. 1, was done the following way [9]. In order to eliminate interference fringes due to the thin film of the pressure medium formed between the sample and the diamond, at each pressure we calculated the ratio of the insulating and metallic phase reflectivity measured usually with 10 K below and above the transition. At $p = 26$ kbar this ratio, obtained as the quotient of the $T = 7$ K and 40 K spectra, is ~ 1 in the whole range verifying the lack of the metal-insulator transition. At pressures smaller than p_{cr} we then evaluated the absolute reflectivity of the insulator according

to

$$R_{abs}^I(p) = \frac{R^I(p)}{R^M(p)} \cdot R_{abs}^M, \quad (1)$$

where $R^I(p)$ and $R^M(p)$ are the raw data obtained at a given pressure below and above T_{MI} , respectively and R_{abs}^M is the out-of-cell ambient pressure metallic curve, which served as a standard. This evaluation does not influence the structure of the spectra since, (i) in the metallic state of BaVS₃ the reflectivity has a weak and monotonic temperature dependence with a relative change $\leq 15\%$ at any of the investigated pressures, and (ii) the high-temperature dc conductivity is not very sensitive to the pressure as $\sigma_{dc}(p = 22 \text{ kbar})/\sigma_{dc}(p = 1 \text{ bar}) \approx 1.2$ at room temperature [8]. After calculating the reflectivity by Eq. 1 some remains of the interference fringes are still superimposed on the data. In order to better visualize the results, we smoothed out this oscillation in the reflectivity by interpolation and then applied the Kramers-Kronig transformation as it is shown in case of the “1 bar”, low temperature measurement in the right panel of Fig. 1. This step effectively lowers the frequency resolution, and it results in the smearing out of the phonon peaks in the range of $200 - 400 \text{ cm}^{-1}$; however, it also allows a better determination of the charge gap. The agreement between the ambient pressure insulating spectra obtained inside and out of the pressure cell is demonstrated in the left panel of Fig. 1.

Above T_{MI} the raw data clearly correspond to metallic behavior: the reflectivity tends $R \rightarrow 1$ approaching zero frequency, as clearly and directly shown in the ambient pressure measurements. In contrast, below T_{MI} the low-frequency reflectivity is constant. Due to the vanishing electronic screening the phonon resonances sharpen. The dominant phonon peak around 100 cm^{-1} is clearly observable below 70 K at ambient pressure and at every pressure as long as the metal to insulator transition takes place. Similarly to the isostructural BaTiS₃ and BaNbS₃ [12], this peak is due to two, closely centered, modes. Both of them correspond to the motion of the barium relative to the sulfur octahedron and the embedded atom (in our case the vanadium). In terms of the optical conductivity, the key finding is the complete suppression of the low-frequency spectral weight below T_{MI} , due to the development of the charge gap. At high frequencies the difference between the metal and the insulator disappears and above $\sim 700 \text{ cm}^{-1}$ all the curves essentially converge. At lower frequency the conductivity goes through a gradual increase and reaches a maximum whose frequency is identified with the gap value (pointed by arrows in Fig. 1). The value of the low-temperature gap at ambient pressure agrees well with the gap derived from the photoemission data of Ref. 11.

The single particle excitations below the gap, if exist, cannot be distinguished from the contribution of a multi-phonon absorption in the $200 - 400 \text{ cm}^{-1}$ range. The

dominance of this phonon branch is visible in case of the ambient pressure measurement [13]. Note that in the same energy scale in-gap impurity states may also give rise to an enhancement of the conductivity.

The charge gap is $\Delta_{ch} \approx 530 \text{ cm}^{-1} = 750 \text{ K}$ at ambient pressure and it is reduced by the applied pressure as the maximum is shifted to lower frequencies. At $p = 26 \text{ kbar}$ neither the opening of the gap nor the sharpening of the 100 cm^{-1} phonons can be detected indicating that the material remains metallic. This is in agreement with the shape of the $p - T$ phase boundary and the value of the critical pressure $p_{cr} \approx 20 \text{ kbar}$ determined by resistivity measurements [8]. As the temperature is lowered, the

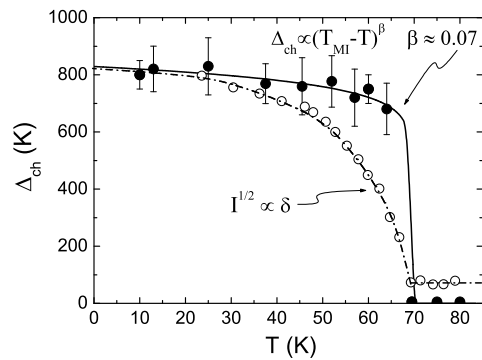


FIG. 2: The solid circles show how the charge gap opens at ambient pressure and the solid curve is the power-law fit on the data below $T_{MI} = 70 \text{ K}$. The open circles are the temperature dependence of the structural distortion measured by Ref. 6. The dashed line represents the BCS function.

onset of the insulating state is rather abrupt, and we observed only a weak change in the reflectivity spectra of the insulator between T_{MI} and $T = 7 \text{ K}$ at any pressure. The temperature dependence of the charge gap is shown in Fig. 2. The opening of the gap can be contrasted with the temperature dependence of the structural distortion, δ measured by Inami *et al.* [6]. Below the transition temperature the intensity of the superlattice reflection was found to linear in $T_{MI} - T$, suggesting that the structural order parameter has a BCS-like temperature dependence, i.e. $\delta(T) \propto \sqrt{T_{MI} - T}$. The onset of the insulating state much more sharp in the charge excitations; 85% of the zero temperature gap is already reached at $T = 0.92 \cdot T_{MI}$. In a wide range below T_{MI} the temperature variation can be described by $\Delta_{ch} \propto (T_{MI} - T)^\beta$ with $\beta = 0.07 \pm 0.013$. In contrast to the optical gap, the activation energy derived from the dc conductivity experiments is influenced by the impurity concentration. In a separate study we have investigated the dc transport of the several samples under pressure. The resistivity of the cleanest sample increased nine order of magnitude from T_{MI} down to $T = 20 \text{ K}$ at ambient pressure. Although its temperature dependence slightly deviates from the Arrhenius law one can estimate the gap within 30% error and find

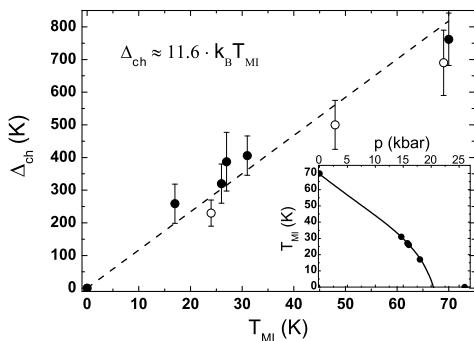


FIG. 3: The charge gap vs. the transition temperature as derived from the optical (solid symbols) and the dc transport (open symbols) experiments. The dashed line corresponds to Eq. 2. The continuous line in the inset is the $p - T$ phase boundary from Ref. 8 and the dots show the pressures investigated in the present study.

$\Delta_{ch} = 690 \pm 100$ K. The magnitude and the pressure dependence of the charge gap determined by IR spectroscopy and dc transport agree fairly well as shown in Fig. 3. In the $p = 0 - 18$ kbar range the following scaling relation holds:

$$\frac{\Delta_{ch}(p)}{k_B T_{MI}(p)} \approx 11.6. \quad (2)$$

Finally, we shortly discuss two basic effects which could be responsible for the large value of the gap parameter, $\Delta_{ch}/k_B T_{MI} \sim 12$. One possibility is that the transition temperature could be much larger, but strong fluctuations suppress the development of the ordered state. When the insulating state develops, the gap rapidly reaches the large value corresponding to the "mean field" transition temperature. In BaVS_3 such fluctuations may be induced by the competition of different orderings like in $\text{La}_{1-x}\text{Ca}_x\text{MnO}_3$ ($x \approx 0.5$) where ferromagnetic and charge order (CO) coexist in a limited region of the $T - x$ phase diagram [1]. A wide precursor range can also arise from the low dimensionality of the system as it is the case in many CDW or SDW compounds or in $\text{La}_{1.67}\text{Sr}_{0.33}\text{NiO}_4$ where the presence of fluctuating charge stripes are observed well above T_{CO} [2]. However, the dynamical fluctuations due to the preexisting short range order are usually manifested in the formation of a pseudogap; this possibility may be excluded by our IR study.

Another explanation is that the charge gap is affected by the electron-electron interaction. Such a correlation-driven enhancement of the gap is thought to be present in several manganites like $\text{Bi}_{1-x}\text{Ca}_x\text{MnO}_3$ ($x = 0.74 - 0.82$) [14], $\text{Pr}_{0.6}\text{Ca}_{0.4}\text{MnO}_3$ [15] and $\text{La}_{1-x}\text{Ca}_x\text{MnO}_3$ ($x \geq 0.6$) and in the nickelate NdNiO_3 [16] where the gap parameter is ~ 20 , ~ 9 , ~ 10 and ~ 20 , respectively. The temperature dependence of the gap in all of the above cited $3d$ compounds fairly follows the BCS functional

form while in BaVS_3 the transition appears in Δ_{ch} in a much sharper manner. In this sense BaVS_3 can rather be related to the spin-Peierls system CuGeO_3 , where a similarly strong temperature dependence of the singlet-triplet gap with an exponent of $\beta \approx 0.1$ is detected by neutron scattering [3]. A microscopic theory describing the metal to insulator transition and the "pressure-magnetic field-temperature" phase diagram [5, 8, 9] of BaVS_3 is highly desirable.

In conclusion, our FIR optical study supplied a detailed experimental description of the evolution of the charge gap in BaVS_3 as a function of pressure and temperature. We have shown the lack of a pseudogap above the phase transition and a strong deviation of $\Delta_{ch}(T)$ from the BCS-type structural order parameter has been found. These results show that BaVS_3 belongs to a novel class of correlated systems where the onset of transition appears in a remarkable different way in the lattice structure and the electron system.

The authors are grateful to P. Fazekas for several indispensable discussions. This work was supported by the Hungarian Research Funds OTKA TS040878, T037451. A part of this work has been carried out at the National Synchrotron Light Source at Brookhaven National Laboratory, which is supported by the U.S. Department of Energy, Division of Materials Sciences and Division of Chemical Sciences, under Contract No. DE-AC02-98CH10886.

-
- [1] K. H. Kim, S. Lee, T. W. Noh, and S.-W. Cheong, Phys. Rev. Lett. **88**, 167204 (2002).
 - [2] T. Katsufuji, T. Tanabe, T. Ishikawa, Y. Fukuda, T. Arima, and Y. Tokura, Phys. Rev. B **54**, 14230 (1996).
 - [3] Michael C. Martin, G. Shirane, Y. Fujii, M. Nishi, O. Fujita, J. Akimitsu, M. Hase, and K. Uchinokura, Phys. Rev. B **53**, R14713 (1996).
 - [4] G. Mihály, I. Kézsmárki, F. Zámorszky, M. Miljak, K. Penc, P. Fazekas, H. Berger, and L. Forró, Phys. Rev. B **61**, R7831 (2000).
 - [5] I. Kézsmárki, Sz. Csonka, H. Berger, L. Forró, P. Fazekas, and G. Mihály, Phys. Rev. B **63**, R81106 (2001).
 - [6] T. Inami, K. Ohwada, H. Kimura, M. Watanabe, Y. Noda, H. Nakamura, T. Yamasaki, M. Shiga, N. Ikeda, and Y. Murakami, Phys. Rev. B **66**, 73108 (2002).
 - [7] T. Graf, D. Mandrus, J. M. Lawrence, J. D. Thompson, P. C. Canfield, S. W. Cheong, and L. W. Rupp, Phys. Rev. B **51**, 2037 (1995).
 - [8] L. Forró, R. Gaál, H. Berger, P. Fazekas, K. Penc, I. Kézsmárki, and G. Mihály, Phys. Rev. Lett. **85**, 1938 (2000).
 - [9] A more elaborated discussion revealing the analogy with spin-Peierls systems and a detailed analysis of the optical spectra measured under pressure is given in I. Kézsmárki, Ph.D. Thesis (2003), <http://dept.phy.bme.hu/~kezsmark/thesis.pdf>.
 - [10] In our notation Δ_{ch} is the entire energy needed for the

charge excitation, not its half. The same convention is followed in case of the spin gap, Δ_{sp} .

- [11] M. Nakamura, A. Sekiyama, H. Namatame, A. Fujimori, H. Yoshihara, T. Ohtani, A. Misu, and M. Takano, Phys. Rev. B **49**, 16191 (1994).
- [12] M. Ishii and M. Saeki, Phys. Status Solidi B **170**, K49 (1992).
- [13] In contrast to the vibrations at $\sim 100 \text{ cm}^{-1}$, only the vanadium and the surrounding sulfur octahedron are involved in these excitations. The highest energy phonon in this branch (appearing at 350 cm^{-1} in BaVS_3) has the largest oscillatory strength. In the two isostructural materials the spectrum are even more dominated by this mode.
- [14] H. L. Liu, S. L. Cooper, and S-W. Cheong, Phys. Rev. Lett. **81**, 4684 (1998).
- [15] Y. Okimoto, Y. Tomioka, Y. Onose and Y. Otsuka, and Y. Tokura, Phys. Rev. B **57**, R9377 (1998).
- [16] T. Katsufuji, Y. Okimoto, T. Arima, Y. Tokura, and J. B. Torrance, Phys. Rev. B **51**, 4830 (1995).